International Journal of Engineering Research & Technology (IJERT)
ISSN: 2278-0181
Vol. 3 Issue 6, June - 2014

# Study of Natural Convection of Heat Transfer in A Vertical Cone Embedded with Porous Medium

N. Ameer Ahamad
Department of Mathematics, Faculty of Science,
P.O.Box 741, University of Tabuk,
Zip. 71491, Kingdom of Saudi Arabia

***Abstract*: In this paper, we concentrate on the study of natural convection of heat transfer confined in a vertical cone embedded with porous medium. Finite Element Method (FEM) has been used to solve the governing partial differential equations. Results are presented in terms of average Nusselt number ($\overline{Nu}$), streamlines and Isothermal lines for various values of Rayleigh number (Ra), Cone angle ($C_A$) & Radius ratio ($R_r$).**

***Keywords:* Porous medium, Nusselt number ($\overline{Nu}$), Rayleigh number (Ra), Cone angle ($C_A$) & Radius ratio ($R_r$).***

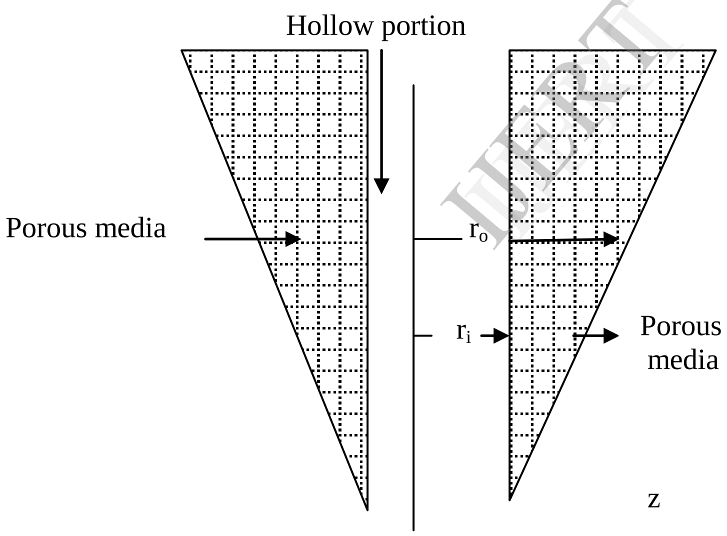




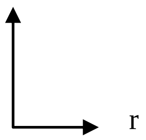


Fig. (A) : Schematic diagram of Vertical Cone Filled with porous medium

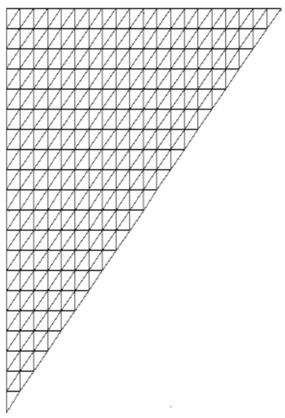

Fig. (B) Mesh Pattern of Vertical Cone embedded with porous medium

**Nomenclature:**

**List of Symbols:-**

$C_A$ = Cone Angle
$C_p$ = Specific heat
$D_p$ = Particle diameter
g = Gravitational acceleration
$H_t$ = Height of the vertical annular cone
K = Permeability of porous media
P = Pressure
$\overline{Nu}$ = Average Nusselt number
$q_t$ = Total heat flux
r, z = Cylindrical co-ordinates
$\bar{r}$ $\bar{z}$ = Non-dimensional co-ordinates
$r_i$ , $r_o$ = Inner and outer radius
Ra =Rayleigh number
$R_r$ = Radius ratio
$R_d$ = Radiation parameter
T= Temperature
$\bar{T}$ =Non-dimenstional Temperature
u = Velocity in r direction
w = Velocity in z direction

**Greek Symbols:-**

$\alpha$ = Thermal diffusity
$\beta_T$ =Co-efficient of thermal expansion
$\varepsilon$ = Viscous dissipation parameter
$\Delta T$ = Temperature difference
$\sigma$= Stephan Boltzman constant
$\rho$= Density
$\gamma$= Coefficient of Kinematic viscosity
$\mu$=Coefficient of dynamic viscosity
$\phi$= Porosity
$\psi$= Stream function
$\bar{\psi}$ = Non-dimensional stream function

**Subscripts:-**

$\omega$ = Wall
$\infty$ = Conditions at infinity
h = Hot
c = Cold
t = Total



## 1. INTRODUCTION

Natural convective heat transfer in porous media has received considerable attention during the past few decades. This interest can be attributed to its wide range of applications in ceramic processing, nuclear reactor cooling system, crude oil drilling, chemical reactor design, ground water pollution and filtration processes. The work on free convection about a vertical imperiable flat plate are studied by Cheng and Minkowycz [1], Cheng [2], Na and Pop [3] Gorla and Zinalabedini [4]. The vertical cylinder cases are investigated by Minkowycz and Cheng [5], Kumari et.al [6] and Bassom et.al [7] Cheng et al. [8] use the local non-similarity method to analyze the natural convection of Darcian fluid about a cone. External free convection in a porous medium adjacent to heated bodies was analyzed by Nield and Bejan [9], Merkin [10, 11], Minkowycz and Cheng [12, 13, 14], Pop and Cheng [8, 15], Ingham and Pop [16]. All through these studies, it is assumed that the boundary layer approximations are applicable and the coupled sets of governing equations are solved by numerical methods.

In the present work, we study the problem of natural convection of heat transfer in a inverted cone embedded with porous medium . In the case of full cone similarity solutions exist if the prescribed wall temperature or surface heat flux is a power function of distance from the vertex of the inverted cone [8, 9, 17, 18]. Bejan and Khair [19] used Darcy's law to study the vertical natural convective flows driven by temperature and concentration gradients. Nakayama and Hossain [20] applied the integral method to obtain the heat and mass transfer by free convection from a vertical surface with constant wall temperature and concentration. Yih [21] examined the coupled heat and mass transfer by free convection over a truncated cone in porous media for variable wall temperature and variable heat and mass fluxes, Also he [22] applied the uniform transpiration effect on coupled heat and mass transfer in mixed convection about inclined surfaces in porous media for the entire regime. Cheng [23] used an integral approach to study the heat and mass transfer by natural convection from truncated cones in porous media with variable wall temperature and [24] studies the Soret and Dufour effects on the boundary layer flow due to natural convection heat and mass transfer over a vertical cone in a porous medium, saturated with Newtonian fluids with constant wall temperature. Natural convective mass transfer from upward-pointing vertical cones, embedded in saturated porous media, was studied using the limiting diffusion [25]. The natural convection along with an isothermal wavy cone embedded in a fluid-saturated porous medium were presented in [26, 27]. Singh and Queeny [28] applied the integral method to obtain the heat and mass transfer by free convection from a vertical surface with constant wall temperature and concentration. In [17, 18] fluid flow and heat transfer of vertical full cone embedded in porous media were solved by Homotopy analysis method.

## 2. MATHEMATICAL FORMULATION

A vertical annular cone of inner radius $r_i$ and outer radius $r_0$ as depicted by schematic diagram as shown in figure (A) is considered to investigate the heat transfer behavior. The co-ordinate system is chosen such that the r-axis points towards the width and z-axis towards the height of the cone respectively. Because of the annular nature, two important parameters emerge which are Cone angle ($C_A$) and Radius ratio ($R_r$) of the annulus. They are defined as

$C_A = \dfrac{H_t}{r_0 - r_i}$, $\quad R_r = \dfrac{r_0 - r_i}{r_i}$, where $H_t$ is the height of the cone.

The inner surface of the cone is maintained at isothermal temperature $T_h$ and outer surface is at ambient temperature $T_\infty$. It may be noted that, due to axisymmetry, a section of the annulus is sufficient for analysis purpose.

We assume that the flow inside the porous medium is assumed to obey Darcy law and there is no phase change of fluid. The properties of the fluid and porous medium are homogeneous, isotropic and constant except for variation of fluid density with temperature. The fluid and porous medium are in thermal equilibrium.

Continuity equation: $$\frac{\partial(ru)}{\partial r} + \frac{\partial(rw)}{\partial z} = 0 \tag{2.1}$$

The velocity in r and z directions can be described by Darcy law as

Velocity in horizontal direction

$$u = \frac{-K}{\mu}\frac{\partial p}{\partial r} \tag{2.2}$$

Velocity in vertical direction

$$w = \frac{-K}{\mu}\left(\frac{\partial p}{\partial z} + \rho g\right) \tag{2.3}$$

The permeability K of porous medium can be expressed as Bejan (29)

$$K = \frac{D_p^2 \phi^3}{180(1-\phi)^2} \tag{2.4}$$

The variation of density with respect to temperature can be described by Boussinesq approximation as

$$\rho = \rho_\infty [1 - \beta_T (T - T_\infty)] \tag{2.5}$$

Momentum Equation :

$$\frac{\partial w}{\partial r}-\frac{\partial u}{\partial z}=\frac{gK\beta}{\nu}\frac{\partial T}{\partial r} \tag{2.6}$$

Energy equation

$$u\frac{\partial T}{\partial r}+w\frac{\partial T}{\partial z}=\alpha\left(\frac{1}{r}\frac{\partial}{\partial r}\left(r\frac{\partial T}{\partial r}\right)+\frac{\partial^2 T}{\partial z^2}\right) \tag{2.7}$$

The last term in the right hand side of the equation (2.7) represents radiation effect.
The continuity equation (1) can be satisfied by introducing the stream function $\psi$ as

$$u=-\frac{1}{r}\frac{\partial\psi}{\partial z} \tag{2.8}$$

$$w=\frac{1}{r}\frac{\partial\psi}{\partial r} \tag{2.9}$$

The corresponding dimensional boundary conditions are

at $r = r_i$, $T = T_w$, $\psi = 0$ (2.10a)

at $r = r_0$, $T = T_\infty$, $\psi = 0$ (2.10b)

(except at z = 0)

The new parameters arising due to cylindrical co-ordinates system are

Non-dimensional Radius $\bar{r}=\frac{r}{L}$ (2.11a)

Non-dimensional Height $\bar{z}=\frac{z}{L}$ (2.11b)

Non-dimensional stream function $\bar{\psi}=\frac{\psi}{\alpha L}$ (2.11c)

Non-dimensional Temperature $\bar{T}=\frac{(T-T_\infty)}{(T_w-T_\infty)}$ (2.11d)

Rayleigh number $Ra=\frac{g\beta_T \Delta TKL}{\nu\alpha}$ (2.12e)

The non-dimensional equations for the heat transfer in vertical cone are

Momentum equation: $$\frac{\partial^2\bar{\psi}}{\partial\bar{z}^2}+\bar{r}\left(\frac{1}{\bar{r}}\frac{\partial\bar{\psi}}{\partial\bar{r}}\right)=\bar{r}Ra\frac{\partial\bar{T}}{\partial\bar{r}} \tag{2.13}$$

Energy equation :

$$\frac{1}{\bar{r}}\left[\frac{\partial\bar{\psi}}{\partial\bar{r}}\frac{\partial\bar{T}}{\partial\bar{z}}-\frac{\partial\bar{\psi}}{\partial\bar{z}}\frac{\partial\bar{T}}{\partial\bar{r}}\right]=\left(\frac{1}{\bar{r}}\frac{\partial}{\partial\bar{r}}\left(\bar{r}\frac{\partial\bar{T}}{\partial\bar{r}}\right)+\frac{\partial^2\bar{T}}{\partial\bar{z}^2}\right) \tag{2.14}$$

The corresponding non-dimensional boundary conditions are

$$\text{at} \quad \bar{r} = \bar{r}_i , \quad \bar{T}=1 , \quad \bar{\psi} = 0 \tag{2.15}$$

$$\text{at} \quad \bar{r} = \bar{r}_0 , \quad \bar{T}=0 , \quad \bar{\psi} = 0 \tag{2.16}$$

## 3. SOLUTION OF GOVERNING EQUATIONS:

Equations (2.13) and (2.14) are coupled partial differential equations to be solved in order to predict the heat transfer behavior. These equations are solvied by using FEM. A simple 3-noded triangular element is considered.

Applying Galerkin method to momentum equation (2.13) yields:

$$\{R^e\} = -\int_A N^T \left( \frac{\partial^2 \bar{\psi}}{\partial \bar{z}^2} + \bar{r} \frac{\partial}{\partial \bar{r}} \left( \frac{1}{\bar{r}} \frac{\partial \bar{\psi}}{\partial \bar{r}} \right) - \bar{r} Ra \frac{\partial \bar{T}}{\partial \bar{r}} \right) d v \tag{3.1}$$

$$\{R^e\} = -\int_A N^T \left( \frac{\partial^2 \bar{\psi}}{\partial \bar{z}^2} + \bar{r} \frac{\partial}{\partial \bar{r}} \left( \frac{1}{\bar{r}} \frac{\partial \bar{\psi}}{\partial \bar{r}} \right) - \bar{r} Ra \frac{\partial \bar{T}}{\partial \bar{r}} \right) 2\Pi \bar{r} dA \tag{3.2}$$

Where $R^e$ is the residue. Considering the individual terms of equation (3.2)

The differentiation of following term results into

$$\frac{\partial}{\partial \bar{r}} \left( [N^T] \frac{\partial \bar{\psi}}{\partial \bar{r}} \right) = [N^T] \frac{\partial^2 \bar{\psi}}{\partial \bar{r}^2} + \frac{\partial [N^T]}{\partial \bar{r}} \frac{\partial \bar{\psi}}{\partial \bar{r}} \tag{3.3}$$

Thus $$\int_A N^T \frac{\partial^2 \bar{\psi}}{\partial \bar{r}^2} dA = \int_A \frac{\partial}{\partial \bar{r}} \left( [N^T] \frac{\partial^2 \bar{\psi}}{\partial \bar{r}^2} \right) 2\Pi \bar{r} dA - \int_A \frac{\partial [N^T]}{\partial \bar{r}} \frac{\partial \bar{\psi}}{\partial \bar{r}} \tag{3.4}$$

The first term on right hand side of equation (3.4) can be transformed into surface integral by the application of Greens theorem and leads to inter-element requirement at boundaries of an element. The boundary conditions are incorporated in the force vector.

Let us consider that the variable to be determined in the triangular area as "T".

The polynomial function for "T" can be expressed as

$$T = \alpha_1 + \alpha_2 r + \alpha_3 z \tag{3.5}$$

The variable T has the value $T_i$, $T_j$ & $T_k$ at the nodal position i, j & k of the element. The r and z co-ordinates at these points are $r_i$, $r_j$, $r_k$ and $z_i$, $z_j$, $z_k$ respectively. Since $T = N_i T_i + N_j T_j + N_k T_k$ (3.6)

Where $N_i$, $N_j$ & $N_k$ are shape functions given by $$N_m = \frac{a_m + b_m r + c_m z}{2A} \tag{3.7}$$

Making use of (3.7) gives $$\int_A N^T \frac{\partial^2 \bar{\psi}}{\partial \bar{r}^2} 2\Pi \bar{r} dA = -\int_A \frac{\partial N^T}{\partial \bar{r}} \frac{\partial N}{\partial \bar{r}} \begin{bmatrix} \bar{\psi}_1 \\ \bar{\psi}_2 \\ \bar{\psi}_3 \end{bmatrix} dA \tag{3.8}$$

Substitution of (3.7) into (3.8) gives $$= \frac{1}{(2A)^2} \int_A \begin{bmatrix} b_1 \\ b_2 \\ b_3 \end{bmatrix} \begin{bmatrix} b_1 b_2 b_3 \end{bmatrix} \begin{bmatrix} \bar{\psi}_1 \\ \bar{\psi}_2 \\ \bar{\psi}_3 \end{bmatrix} 2\Pi \bar{r} dA$$

$$= -\frac{2\Pi \bar{R}}{4A} \begin{bmatrix} b_1^2 & b_1 b_2 & b_1 b_3 \\ b_1 b_2 & b_2^2 & b_2 b_3 \\ b_1 b_3 & b_2 b_3 & b_3^2 \end{bmatrix} \begin{bmatrix} \bar{\psi}_1 \\ \bar{\psi}_2 \\ \bar{\psi}_3 \end{bmatrix} \tag{3.9}$$

Similarly, $$\int_A N^T \frac{\partial^2 \bar{\psi}}{\partial \bar{z}^2} 2\Pi \bar{r} dA = -\frac{2\Pi \bar{R}}{4A} \begin{bmatrix} c_1^2 & c_1 c_2 & c_1 c_3 \\ c_1 c_2 & c_2^2 & c_2 c_3 \\ c_1 c_3 & c_2 c_3 & c_3^2 \end{bmatrix} \begin{bmatrix} \bar{\psi}_1 \\ \bar{\psi}_2 \\ \bar{\psi}_3 \end{bmatrix} \tag{3.10}$$

The third term of equation (3.2) gives

$$\int_A N^T \bar{r} Ra \frac{\partial \bar{T}}{\partial \bar{r}} 2\Pi \bar{r} dA = Ra \int_A N^T \bar{r} \frac{\partial \bar{T}}{\partial \bar{r}} 2\Pi \bar{r} dA \tag{3.11}$$

Since $M_1 = N_1$, $M_2 = N_2$, $M_3 = N_3$

Where $M_1$, $M_2$ and $M_3$ are the area ratios of the triangle and $N_1$, $N_2$ and $N_3$ are the shape functions.

Replacing the shape functions in the above equation (3.11) gives

$$\int_A N^T \bar{r} Ra \frac{\partial \bar{T}}{\partial \bar{r}} 2\Pi \bar{r} dA = \bar{r} Ra \int_A \begin{bmatrix} M_1 \\ M_2 \\ M_3 \end{bmatrix} \frac{\partial (N)}{\partial \bar{r}} \begin{bmatrix} \bar{T}_1 \\ \bar{T}_2 \\ \bar{T}_3 \end{bmatrix} 2\Pi \bar{r} dA \tag{3.12}$$

$$= Ra \frac{A}{3} \begin{bmatrix} 1 \\ 1 \\ 1 \end{bmatrix} \frac{2\Pi \bar{R}^2}{2A} \begin{bmatrix} b_1 + b_2 + b_3 \end{bmatrix} \begin{bmatrix} \bar{T}_1 \\ \bar{T}_2 \\ \bar{T}_3 \end{bmatrix}$$

$$= \frac{2\Pi \bar{R}^2 Ra}{6} \begin{Bmatrix} b_1 \bar{T}_1 + b_2 \bar{T}_2 + b_3 \bar{T}_3 \\ b_1 \bar{T}_1 + b_2 \bar{T}_2 + b_3 \bar{T}_3 \\ b_1 \bar{T}_1 + b_2 \bar{T}_2 + b_3 \bar{T}_3 \end{Bmatrix} \tag{3.13}$$

Now the momentum equation (3.13) leads to

$$\frac{2\Pi\bar{R}}{4A}\left\{\begin{bmatrix} b_1^2 & b_1b_2 & b_1b_3 \\ b_1b_2 & b_2^2 & b_2b_3 \\ b_1b_3 & b_2b_3 & b_3^2 \end{bmatrix}+\begin{bmatrix} c_1^2 & c_1c_2 & c_1c_3 \\ c_1c_2 & c_2^2 & c_2c_3 \\ c_1c_3 & c_2c_3 & c_3^2 \end{bmatrix}\right\}\begin{Bmatrix} \bar{\psi}_1 \\ \bar{\psi}_2 \\ \bar{\psi}_3 \end{Bmatrix}+\frac{2\Pi\bar{R}^2 Ra}{6}\begin{Bmatrix} b_1\bar{T}_1+b_2\bar{T}_2+b_3\bar{T}_3 \\ b_1\bar{T}_1+b_2\bar{T}_2+b_3\bar{T}_3 \\ b_1\bar{T}_1+b_2\bar{T}_2+b_3\bar{T}_3 \end{Bmatrix}=0 \tag{3.14}$$

Which is in the form of the stiffness matrix

$$[K_s]\{\bar{\psi}\}=\{f\}$$

Similarly application of Galerkin method to Energy equation (2.14) gives

$$\{R^e\}=-\int_A N^T\left[\frac{1}{\bar{r}}\left(\frac{\partial\bar{\psi}}{\partial\bar{r}}\frac{\partial\bar{T}}{\partial\bar{z}}-\frac{\partial\bar{\psi}}{\partial\bar{z}}\frac{\partial\bar{T}}{\partial\bar{r}}\right)-\left(\frac{1}{\bar{r}}\frac{\partial}{\partial\bar{r}}\left(\bar{r}\frac{\partial\bar{T}}{\partial\bar{r}}+\frac{\partial^2\bar{T}}{\partial\bar{z}^2}\right)\right)\right]2\Pi\bar{r}dA \tag{3.15}$$

Considering the terms individually of the above equation (3.15)

Thus the stiffness matrix of Energy equation (2.14) is given by:

$$\left[\frac{2\Pi}{12A}\begin{Bmatrix} c_1\bar{\psi}_1+c_2\bar{\psi}_2+c_3\bar{\psi}_3 \\ c_1\bar{\psi}_1+c_2\bar{\psi}_2+c_3\bar{\psi}_3 \\ c_1\bar{\psi}_1+c_2\bar{\psi}_2+c_3\bar{\psi}_3 \end{Bmatrix}[b_1,b_2,b_3]-\frac{2\Pi}{12A}\begin{Bmatrix} b_1\bar{\psi}_1+b_2\bar{\psi}_2+b_3\bar{\psi}_3 \\ b_1\bar{\psi}_1+b_2\bar{\psi}_2+b_3\bar{\psi}_3 \\ b_1\bar{\psi}_1+b_2\bar{\psi}_2+b_3\bar{\psi}_3 \end{Bmatrix}[c_1,c_2,c_3]\right]\begin{bmatrix} \bar{T}_1 \\ \bar{T}_2 \\ \bar{T}_3 \end{bmatrix}$$
$$+\frac{2\Pi\bar{R}}{4A}\left\{\begin{bmatrix} b_1^2 & b_1b_2 & b_1b_3 \\ b_1b_2 & b_2^2 & b_2b_3 \\ b_1b_3 & b_2b_3 & b_3^3 \end{bmatrix}\begin{bmatrix} \bar{T}_1 \\ \bar{T}_2 \\ \bar{T}_3 \end{bmatrix}+\begin{bmatrix} c_1^2 & c_1c_2 & c_1c_3 \\ c_1c_2 & c_2^2 & c_2c_3 \\ c_1c_3 & c_2c_3 & c_3^2 \end{bmatrix}\begin{bmatrix} \bar{T}_1 \\ \bar{T}_2 \\ \bar{T}_3 \end{bmatrix}\right\}=0 \tag{3.16}$$



## 4. RESULTS AND DISCUSSION:

Results are obtained in terms of the average Nusselt number ($\overline{Nu}$) at hot wall for various parameters such as Rayleigh number(Ra), Cone angle ($C_A$), Rayleigh number (Ra) and Radius ratio ($R_r$) when heat is supplied to vertical cone embedded with porous medium.

The average Nusselt number ($\overline{Nu}$), is given by $\overline{Nu} = \int_0^{\bar{z}}\left(\frac{\partial\bar{T}}{\partial\bar{r}}\right)$

ISSN: 2278-0181
Vol. 3 Issue 6, June - 2014

a)

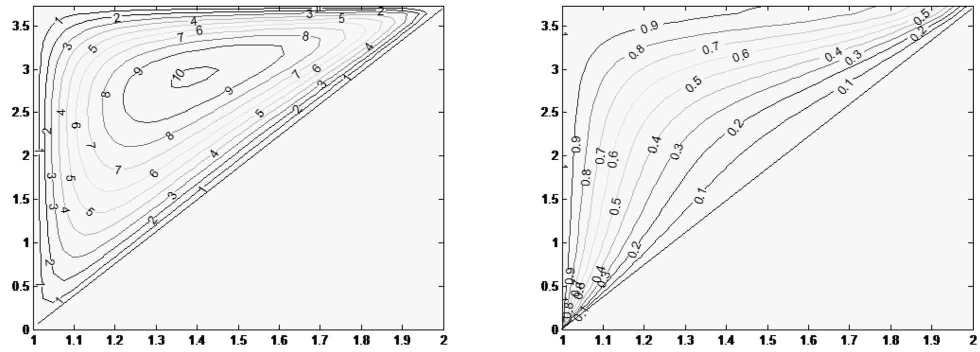

b)

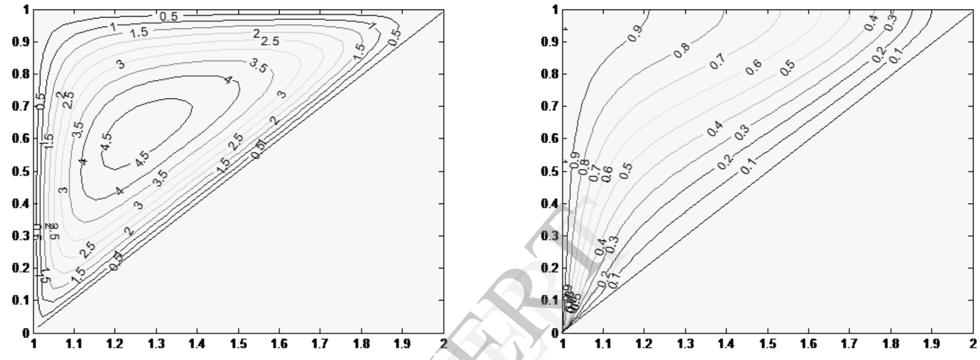

c)

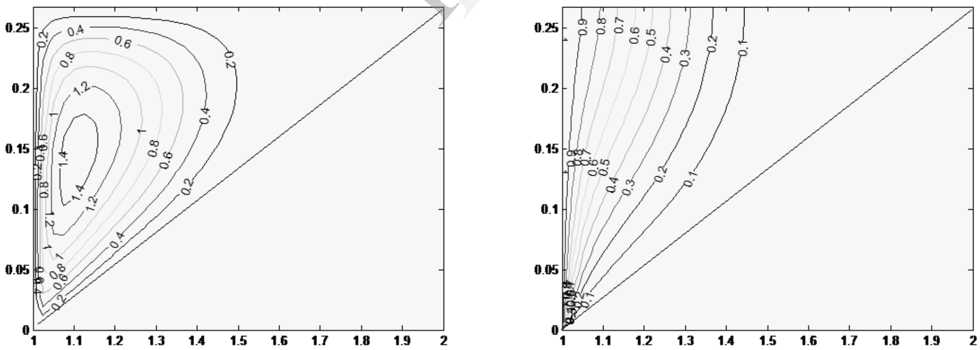



Fig: 2. Streamlines (left) and Isotherms(Right) for Ra=100, $R_r$=1
a) $C_A$ =15 b) $C_A$ =45 c) $C_A$ =75

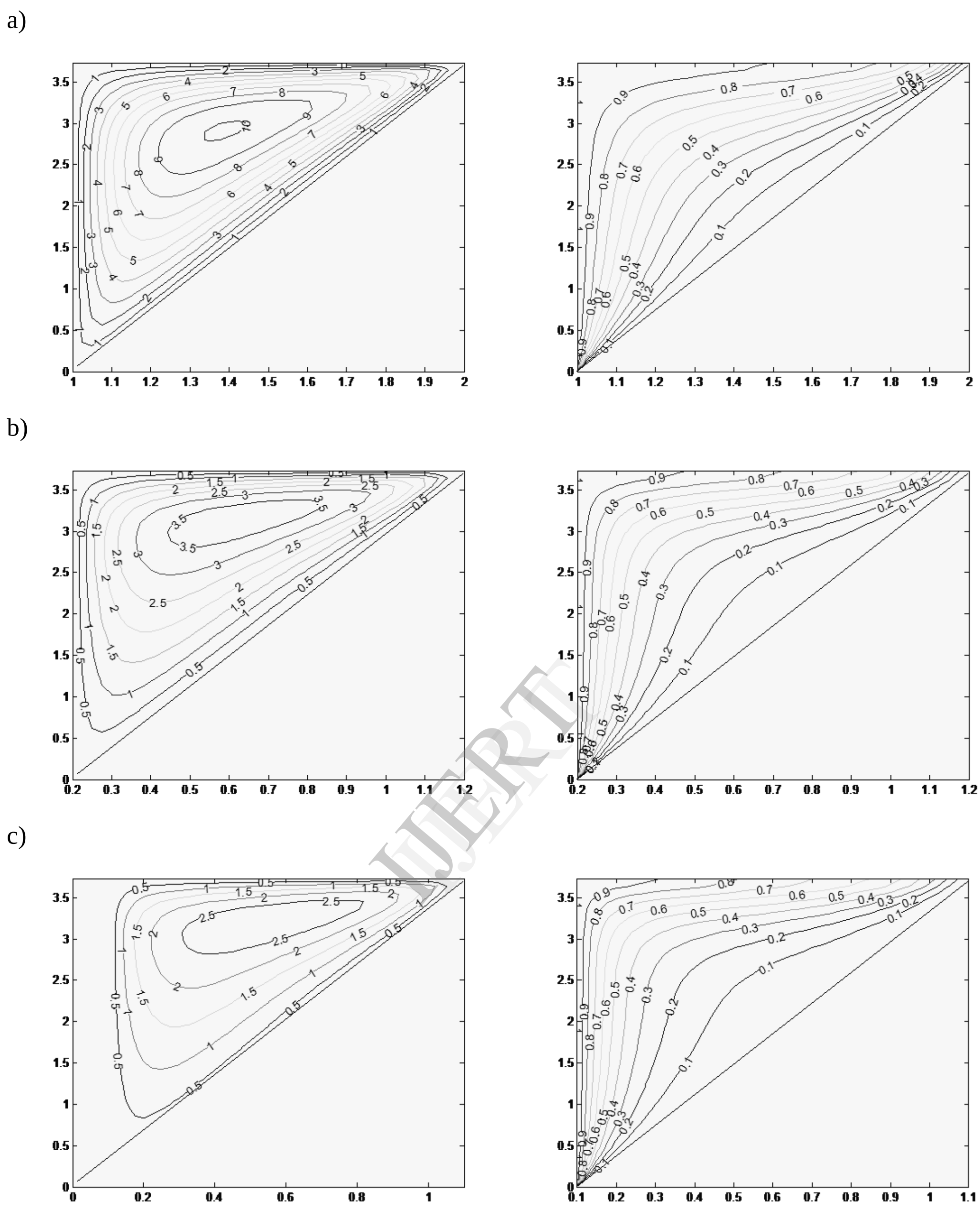


Fig: 2. Streamlines (left) and Isotherms (Right) for Ra=100, $C_A$ =15
a) $R_r$=1 b) $R_r$=5 c) $R_r$=10

a)

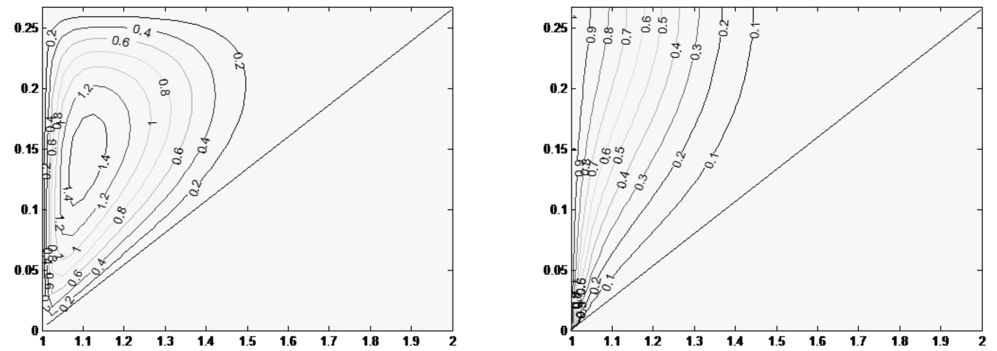


b)

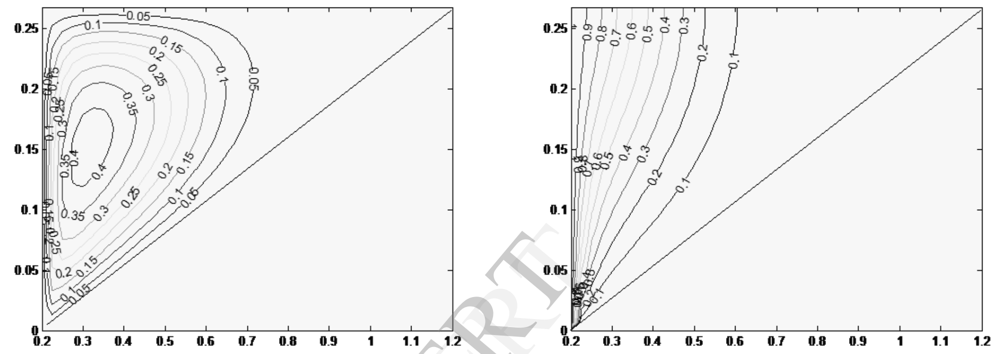


c)

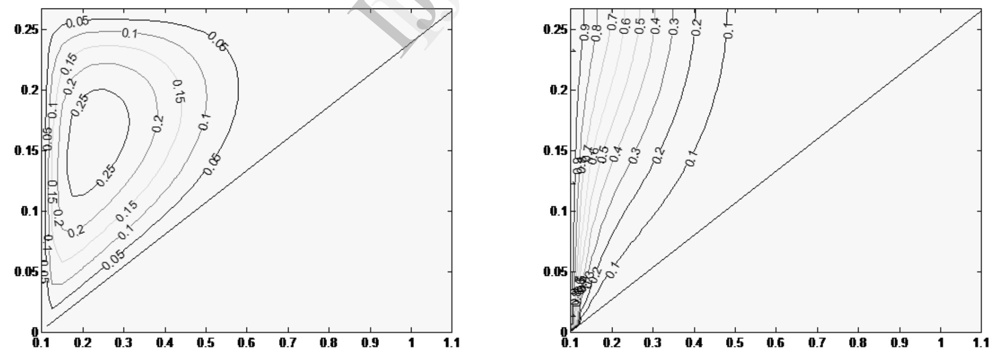




Fig:3. Streamlines(left) and Isotherms (Right) for Ra=100, $C_A$ =75
a) $R_r$=1 b) $R_r$=5 c) $R_r$=10

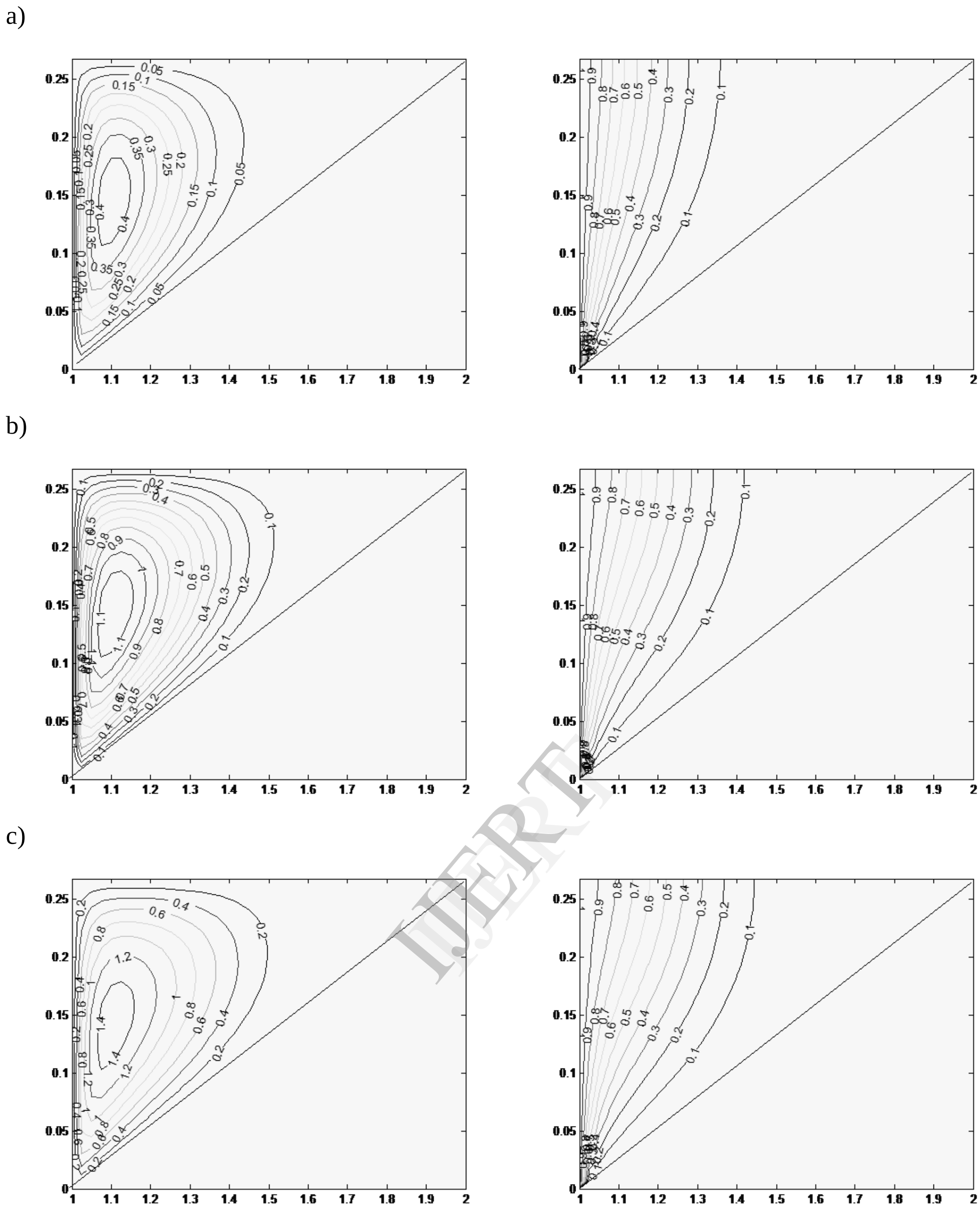

Fig:4. Streamlines(left) and Isotherms (Right) for $C_A$ =75, $R_r$=1
a) Ra=25 b) Ra=75 c) Ra=100



Fig.1 shows the evaluation of streamlines and isothermal lines inside the porous medium for various values of Cone angle ($C_A$) at Ra = 100, $R_r$ = 1. The magnitude of the streamlines decreases with the increase in Cone angles($C_A$), this is because the thermal bounded layer thickness decreases with the increase of Cone angles ($C_A$). It can be seen from streamlines and isothermal lines that the fluid movements shifts from lower portion of the hot wall to upper portion of the cold wall of the vertical annual cone with the increase of Cone angles ($C_A$). The circulation of the fluid covers almost whole domain at both lower and higher values of Cone angles ($C_A$) at $15^o$. Where the relation inversely proportion exists between streamlines and Cone angles ($C_A$). This trend is also observed with isothermal lines.

Fig.2 predicts the streamlines and isothermal lines inside the porous medium for various values of Radius ratio ($R_r$) at Ra = 100 and $C_A$ = 15. It can be observed that be horizontal scale changes for various values of Radius Ratio($R_r$). The magnitude of the streamlines decrease with the increase in Radius ratio ($R_r$). The thermal boundary layer thickness decreases with the increase in Radius ratio ($R_r$). It can be seen from the streamlines and isothermal lines that the fluid movement shifts from lower portion of the hot wall to the upper portion of the cold of the vertical annular cone with the increase in Radius ratio ($R_r$). The circulation of fluid covers almost whole domain at both lower and higher values of Radius ratio ($R_r$).

Fig.3 analysis the streamlines and isothermal lines inside the porous medium for various values of Radius ratio ($R_r$) at Ra = 100 and $C_A$ = 75. It is seen that the streamlines and the isothermal lines tends to move away from the cold wall and reaches nearer to the hot wall of the vertical annular cone. The thermal boundary layer becomes thinner with the increasing Radius ratio ($R_r$).

Fig.4 indicates the streamlines and isothermal lines inside the porous medium for various values of Rayleigh number (Ra) at $C_A$ = 75 and $R_r$ = 1. The thermal boundary layer becomes thinner with the increase Rayleigh number (Ra). So, the streamlines and isothermal lines tends to move away from the cold wall and reaches nearer to the hot wall of the vertical annular cone.

Fig.5 illustrates the effect of Rayleigh number (Ra) on the average Nusselt number ($\overline{Nu}$). This Figure is obtained for value of $R_r$ = 1. When cone angle is increased from 15 to 75, at the hot wall of the vertical annular cone, it is found that the average Nusselt number ($\overline{Nu}$)at Ra = 10 is increased by 23.3%. The corresponding increase in average Nusselt number ($\overline{Nu}$) at Ra =100 is found to be 26.3%. The difference between the average Nusselt number ($\overline{Nu}$) at two different values of Cone angle ($C_A$) increases with increase in Cone angle ($C_A$). This is due to the reason that high cone angle produces high buoyancy force, which leads to increased fluid movements and thus increased the average Nusselt number ($\overline{Nu}$)with Rayleigh number (Ra) as expected. This increase is almost linear for Cone angles ($C_A$) 15 & 45 degrees.

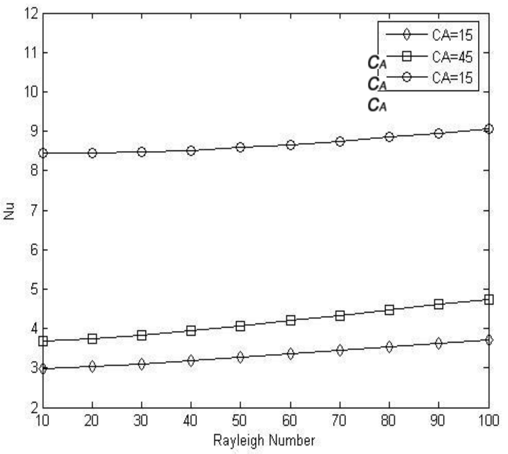


Fig.5 $\overline{Nu}$ variation with Ra at hot surface for different values of $C_A$ at I

Fig.6 shows the variation of average Nusselt number ($\overline{Nu}$)at hot wall with respect to Rayleigh number (Ra). This Figure is obtained for the value of $C_A$ = 75. When Radius ratio ($R_r$) is increased from 1 to 10 at the hot wall of the vertical annular cone, it is found that the average Nusselt number ($\overline{Nu}$) at Ra = 10 is increased by 20%. The corresponding increases in average Nusselt number ($\overline{Nu}$) at Ra = 100 is found to be 21%. The difference between the average Nusselt number ($\overline{Nu}$) at two difference values of Radius ratio ($R_r$) increases with increase in Radius ratio ($R_r$). High Radius ratio ($R_r$) produces high buoyancy force, which leads to faster fluid movements and thus increased the average Nusselt number ($\overline{Nu}$). i.e., for a given Rayleigh number (Ra) Nusselt number ($\overline{Nu}$) increases with Radius ratio ($R_r$).

Fig.7 illustrates the effect of Radius ratio ($R_r$) on the average Nusselt number ($\overline{Nu}$).This Figure corresponds to the value Ra = 100. It is seen that the average Nusselt number ($\overline{Nu}$) at hot wall of the vertical annular cone increases with increase in Radius ratio ($R_r$). It is found that the average Nusselt number ($\overline{Nu}$) at $R_r$ = 1 increased by 9.2% when Cone angle ($C_A$) increased from 15 to 45. The corresponding increase in average Nusselt number ($\overline{Nu}$) at Rr = 10 is found to be 9.8%. This difference between the average Nusselt number ($\overline{Nu}$) at two different value of Cone angle ($C_A$) increases with increase Cone angle ($C_A$). This difference becomes more prominent with the increase in Radius ratio ($R_r$) for higher values of Cone angle ($C_A$).

Fig.8 shows the variation of average Nusselt number ($\overline{Nu}$) at hot wall with respect to Radius ratio ($R_r$). This Figure is obtained for the value of $C_A$ = 75. The average Nusselt number ($\overline{Nu}$) at hot wall of the vertical annular cone increases with increase in Radius ratio ($R_r$). It is found that the average Nusselt number ($\overline{Nu}$) at $R_r$ = 1 increases by 5.8% when Rayleigh number (Ra) is increased from 25 to 100. The corresponding increase in average Nusselt number ($\overline{Nu}$) at $R_r$ = 10 is found to be 10.8%. This difference between the average Nusselt number ($\overline{Nu}$) at Rayleigh number (Ra) increase with increase in Rayleigh number (Ra). This difference increases with increase in Radius ratio ($R_r$) for higher value of Rayleigh number (Ra). The nonlinearity of the curves increases as Rayleigh number (Ra) increases indicating higher curvature activity in the cavity.

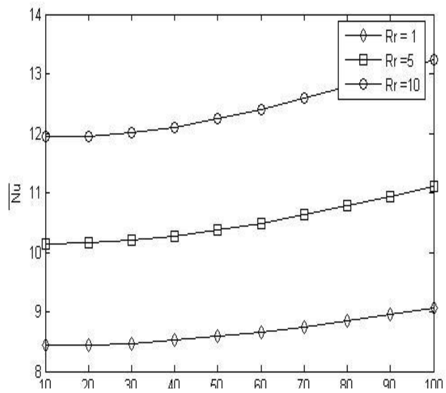


Fig.6 $\overline{Nu}$ variation with Ra at hot surface for different values of $R_r$ at $C_A$ = 75

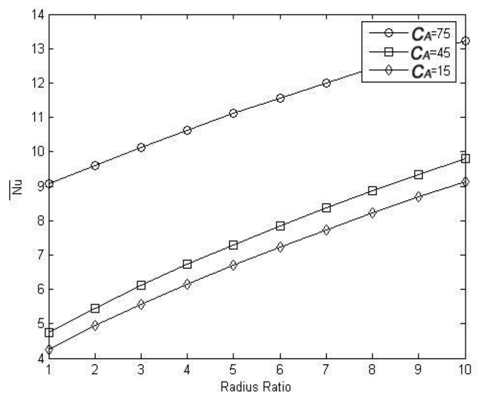


Fig.7 $\overline{Nu}$ variation with $R_r$ at hot surface for different values of $C_A$ at Ra = 100

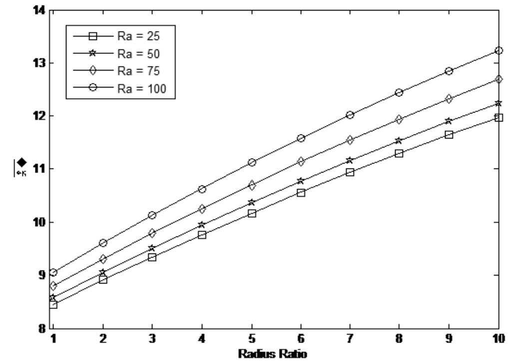


Fig.8 $\overline{Nu}$ variations with $R_r$ at hot surface for different values of Ra at $C_A$ = 75

## 5. REFERENCES


[1] P. Cheng, W. J. Minkowycz, Free convection about a vertical flat plate embedded in a porous medium with application to heat transfer from a dike, Journal of Geophysical Research, Vol.82, No.14, ( 1977), pp. 2040–2044.

[2] P. Cheng, Constant surface heat flux solutions for porous layer flows, (Lett.) Heat Mass Transfer, Vol. 4 (1977), pp. 119–128.

[3] T.Y.Na and I.Pop, Free convection flow past a vertical flat plate embedded in a saturated porous medium, International Journal of Engineering Sciences, Vol.21, No.5, (1983), pp.517-526.

[4] R. S. R. Gorla and A. H. Zinalabedini, "Free convection from a vertical plate with non-uniform surface temperature and embedded in a porous medium," *Journal of Energy Resources Technology*, Vol. 109, No.1, (1987), pp. 26–30.

[5] W.J.Minkowycz and P. Cheng., Free Convection about a Vertical Cylinder embedded in a Porous Medium, International Journal of Heat and Mass Transfer, Vol.19, (1976), pp. 805 – 813.

[6] M. Kumari, I. Pop*, G. Nath, Finite-difference and improved perturbation solutions for free convection on a vertical cylinder embedded in a saturated porous medium, International Journal of Heat and Mass Transfer, Vol. 28, No. 11, (1985), pp.2171–2174.

[7] A.P. Bassom and D.A.S. Ress, Free convection from a heated vertical cylinder embedded in a fluid-saturated porous medium, Acta Mechanica, Vol.116, (1996), pp.139-151.

[8] P. Cheng, T.T. Le and I. Pop., International Communication in Heat and Mass Transfer, Vol-12, (1985), pp.705 –717.

[9] DA. Nield, A. Bejan. Convection in Porous Media, third ed., Springer-Verlag, New York, (2006).

[10] J. H. Merkin, Free convection boundary layers in a saturated porous medium with lateral mass flux, International Journal of Heat and Mass Transfer, Vol. 21, (1978), pp. 1499-1504.

[11] J. H. Merkin, Free convection boundary layers on axisymmetric and two dimensional bodies of arbitrary shape in a saturated porous medium, International Journal of Heat and Mass Transfer, Vol. 22, (1979), pp. 1461-1462.

[12] WJ. Minkowycz, P. Cheng, Free convection about a vertical cylinder embedded in a porous medium, International Journal of Heat and Mass Transfer , Vol.19, (1976), pp. 805-813.

[13] WJ. Minkowycz, P. Cheng, Local non-similar solutions for free convective flow with uniform lateral mass flux in a porous medium, Letters in Heat and Mass Transfer , Vol.9, (1982), pp. 159-168.

[14] WJ. Minkowycz, P. Cheng, F. Moalem, The effect of surface mass transfer on buoyancy induced Darcian flow adjacent to a horizontal heated surface. International Communications in Heat and Mass Transfer, Vol. 12, (1985), pp. 55-65.

[15] I. Pop, P. Cheng, An integral solution for free convection of a Darcian fluid about a cone with curvature effects, International Communications in Heat and Mass Transfer ,Vol.13, (1986), pp.433-438.

[16] DB. Ingham, I. Pop, Natural convection about a heated horizontal cylinder in a porous medium, The Journal of Fluid Mechanics, Vol.184, (1987), pp. 157-181.

[17] AR. Sohouli, D. Domairry, M. Famouri, A. Mohsenzadeh, Analytical solution of natural convection of Darcian fluid about a vertical full cone embedded in porous media prescribed wall temperature by means of HAM, International Communications in Heat and Mass Transfer, Vol. 35, (2008), pp. 1380-1384.

[18] AR. Sohouli, M. Famouri, A. Kimiaeifar, G. Domairry, Application of homotopy analysis method for natural convection of Darcian fluid about a vertical full cone embedded in pours media prescribed surface heat flux, Communications in Nonlinear Science and Numerical Simulation , Vol.15, (2010), pp. 1691-1699.

[19] A. Bejan, KR. Khair, Heat and mass transfer by natural convection in a porous medium, International Journal of Heat and Mass Transfer, Vol. 28, (1985), pp.909-918.

[20] A. Nakayama, MA. Hossain, An integral treatment for combined heat and mass transfer by natural convection in a porous medium, International Journal of Heat and Mass Transfer, Vol. 38, (1995), pp. 761-765.

[21] KA. Yih, Coupled heat and mass transfer by free convection over a truncated cone in porous media: VWT/VWC or VHF/VMF, Acta Mechanica, Vol.137, (1999), pp. 83-97.

[22] KA. Yih, Uniform transpiration effect on coupled heat and mass transfer in mixed convection about inclined surfaces in porous media: the entire regime, Acta Mechanica , Vol.132, (1999), pp. 229-240.

[23] CY. Cheng, An integral approach for heat and mass transfer by natural convection from truncated cones in porous media with variable wall temperature and concentration, International Communications in Heat and Mass Transfer, Vol.27, (2000), pp. 437-548.

[24] CY. Cheng, Soret and Dufour effects on natural convection heat and mass transfer from a vertical cone in a porous medium, International Communications in Heat and Mass Transfer, Vol.36, (2009), pp. 1020-1024.

[25] SU. Rahman, K. Mahgoub, A. Nafees, Natural Convective Mass Transfer from Upward Pointing Conical Surfaces in Porous Media, Chemical Engineering Communications, Vol. 194, (2007), pp.280-290.

[26] I. Pop, T. Y. Na, Naturnal convection of a Darcian fluid about a wavy cone, InternationalCommunications in Heat and Mass Transfer, Vol,21, (1994), pp. 891-899.

[27] I. Pop, T. Y. Na, Natural convection over a frustum of a wavy cone in a porous medium, Mechanics Research Communications, Vol. 22, (1995), pp. 181-190.

[28] P.Singh, Queeny, Free Convection heat and mass transfer along a vertical surface in a porous medium, Vol, 123, (1997), pp.69-73.

[29] A. Bejan, "Convective Heat Transfer", 2nd Edition, New York, John Wiley & Sons (1995).

[30] R.W. Lewis, P. Nithiarasu and K.N. Seetharamu "Fundamentals of the finite element method for heat and fluid flow. John Wiley and Sons, Chichester (2004).
[31] L.J. Seger land, "Applied Finite Element Analysis" John Wiley & Sons, New York (1982).
[32] R.W. Clugh, "The Finite Element Analysis in plane stress Analysis" Proc. 2nd ASCE conf. on Electronic computation, Pittsburg, PA.
[33] O.C. Zinkiewicz and K. Cheng, "Finite Element in the solution of field problems" Engineer, Vol. 24, (1965), pp. 507-510.
[34] J.N.Reddy, An introduction to the Finite Element Method, 2nd Ed., McGraw-Hill, New York, 1993.
[35] S.S. Rao, The Finite Element Method in Engineering, 4th Ed., Elsevier Science & Technology, 2004.